



Science Arts & Métiers (SAM)

is an open access repository that collects the work of Arts et Métiers Institute of Technology researchers and makes it freely available over the web where possible.

This is an author-deposited version published in: <https://sam.ensam.eu>
Handle ID: <http://hdl.handle.net/10985/8434>

To cite this version :

Carl E. CROSS, Nicolas CONIGLIO - Coherency and Grain Size Effects on Solidification Crack Growth in Aluminum Welds - Materials Testing - Vol. 7/8, n°56, p.583-590 - 2014

Any correspondence concerning this service should be sent to the repository

Administrator : scienceouverte@ensam.eu



Coherency and Grain Size Effects on Solidification Crack Growth in Aluminum Welds

Nicolas Coniglio, Aix en Provence,
France and Carl E. Cross,
Los Alamos, USA

Article Information

Correspondence Address

Prof. Dr. Carl E. Cross
Los Alamos National Laboratory, Materials
Science & Technology, P.O. Box 1663,
MS: G770, Los Alamos, NM, 87545 USA
E-mail: cecross@lanl.gov

Keywords

Aluminium welding, solidification cracking,
critical strain rate, coherency point, grain size

A mass balance model has been evaluated that estimates the critical conditions for sustaining continuous crack growth in the mushy weld zone. With the aid of a strain partition model, the critical local strain rate (across the weld) has been related to the critical grain boundary deformation rate needed for crack growth. In the present work, these two models are applied to aluminum welds to investigate the theoretical effects of several metallurgical factors on solidification cracking susceptibility. Calculations quantify the improved cracking resistance associated with a smaller coherent temperature range, grain refinement, high solid fraction at coherency, and rapid development of tensile strength through solid-solid bonding.

Certain aluminum alloys are particularly susceptible to solidification cracking during welding. The occurrence of this cracking remains a poorly understood phenomenon, not possible to predict, in spite of extensive experimental studies and modeling. Solidification cracking is generally believed to result from the uniaxial tensile fracture of liquid films at grain boundaries within the two-phase mushy zone [1]. Stresses and strains at the trailing edge of the weld pool can be either compressive or tensile, and arise from an interaction between the weld thermal experience (i.e., heating and cooling cycles), restraining forces, and solidification shrinkage [2-4].

Compression cells form as a result of localized heating (restrained expansion), whereas tensile cells form in reaction to this compression, but also include stresses resulting from rapid cool down (restrained contraction) plus solidification shrinkage. When examining the conditions needed for a weld solidification crack to exist, one must consider both crack nucleation and growth, although in either case the associated mechanisms are not well defined. Crack nucleation involves the creation of a liquid vapor interface, i.e., liquid fracture [1], from which a crack may then grow un-

der favorable conditions that require the presence of a tensile stress.

Solidification cracking in general has been viewed in a great diversity of ways [5-8]. Its occurrence in welds, for example, has been defined in terms of critical stresses, strains, and strain rates [9, 10]. While some cracking models consider the maximum stress a liquid film can sustain [11-13], most assume that fracture in the mushy zone is strain limited [14-16]. Arguing that a large solidification range permits a large build-up of strain and a greater likelihood to crack [17, 18], it has been demonstrated that cracking will occur if the accumulated strain exceeds a ductility limit represented by characteristic ductility curves established for specific alloys. Ductility-based models have recognized that strain rate is also an important factor, but only in so far as it serves to determine how much strain can be accumulated during the time of solidification [16]. A majority of these models suffer from one common shortfall in that they fail to address how the liquid is fractured. One notable exception to this is the recent model of Rappaz, Drezet and Gremaud (RDG) [19], where liquid fracture is specifically related to an interdendritic pressure drop and cavitation.

However, recent application of this model to aluminum welds has suggested that conditions for cavitation require anomalously high amounts of dissolved gas in the interdendritic liquid [20].

Mechanisms for solidification crack growth have received only limited attention in the literature. Following nucleation of the solidification crack, specific conditions are required to grow the crack, in terms of stress [21, 22] or strain rate [20, 23-26]. Stress-based models have been used to characterize crack growth by applying solid-state fracture mechanisms to liquid film rupture, taking into account surface energy effects [21] and a modified Griffith criterion [22]. One pressure-based model assumes a gas pore to grow as a crack if the sum of pressures contributing to its growth (e.g., liquid pressure drop and dissolved gas pressure) exceeds the pressures contributing to its shrinkage (hydrostatic pressure, capillary pressure, atmospheric pressure) [24]. A simplified mass balance approach [20, 25, 26] considers the crack opening due to transverse deformation to be compensated by advancement of the crack and feeding of liquid. Of particular interest to welding is the boundary condition that crack growth is fixed at the weld-

ing speed, where the crack tip must remain in the mushy zone [20, 27, 28].

Important to solidification cracking modeling is the concept of coherency, which is a unique property of the alloy and solidification conditions [9]. Coherency corresponds to the interconnection of the dendrite arms, either mechanically (interlocking) or through atomic bonding, and is accompanied by a marked increase in shear strength below the coherency temperature [29-31]. The solid fraction interval in which coherency exists determines how solidification shrinkage will be distributed in the mushy zone. The ability to feed shrinkage with liquid diminishes with solid fraction, causing a pressure drop. At later stages of solidification, where liquid is no longer continuous, there is a rapid build-up of tensile strength. The ability to support a tensile stress is an important aspect needed for crack growth. That being said, the typical smooth appearance of the solidification crack fracture surfaces suggests that crack growth seldom involves the tearing of dendrites, but rather involves the continuous separation of a liquid film.

In the present work it is assumed that a crack has already nucleated and thus only conditions required for continuous crack growth will be examined. It is considered reasonable to assume that the nucleation of cracks will not be a controlling step, based upon the abundance of liquid vapor defects already present in the weld pool including porosity and oxide biofilms [1, 20]. The aim of this publication is to apply a mass balance approach to estimate the effects of coherent temperature range, grain size, solid

fraction at coherency, and crack tip location upon the conditions required to promote steady-state growth of a solidification crack.

Solidification Crack Modeling

Crack Growth Model. The mass balance based crack growth model presented here has been developed in more detail in a previous work [20]. When evaluating crack growth, the mass balance approach was deemed particularly applicable to the steady-state conditions of continuous crack advancement behind the weld pool. Specifically, the crack grows continuously in liquid that is present at a grain boundary, with its tip located at a fixed position within the mushy zone at a fixed solid fraction.

Grains in the mushy zone are considered separated by a liquid film of thickness h as depicted in Figure 1. $(L-x)$ is taken as the length of liquid film exposed to transverse strain in the region of dendrite coherency. The transverse deformation rate $\dot{\delta}_L$ is compensated by both advancement of the crack (rate \dot{x} equal to weld travel speed) and liquid feeding (flow rate v_L) in the form of a mass balance:

$$\dot{\delta}_L(L-x) = \dot{x}h_1 + v_L h_2 \quad (1)$$

with h_1 , h_2 : liquid film thickness at the crack tip and coherency point positions. At a solid fraction f_s , the liquid film thickness h equals $(1-f_s) \times \lambda_1$, where λ_1 is primary dendrite arm spacing.

The RDG model [19] estimates the interdendritic liquid pressure drop at the dendrite root (ΔP_{\max}) due to insufficient liquid

feeding to compensate solidification shrinkage and thermal contraction:

$$\Delta P_{\max} = P_L - P_0 = \Delta P_e + \Delta P_{sh} =$$

$$\frac{(1+\beta)\mu}{G} \int_{T_s}^{T_L} \frac{E(T)}{K} dT + \frac{v_T \beta \mu}{G} \int_{T_s}^{T_L} \frac{1-f_s(T)}{K} dT \quad (2)$$

$$\text{with } E(T) = \frac{1}{G} \int_{T_s}^T f_s(T) \dot{E}(T) dT$$

P_L and P_0 : liquid pressure at dendrite tip and root, μ is liquid viscosity, β is shrinkage factor, v_T is isotherm velocity, G is thermal gradient, T_s and T_L are solidus and liquidus temperatures, K is dendrite permeability, and $f_s(T)$ and $\dot{E}(T)$ are solid fraction and strain rate at temperature T , respectively.

The first term on the right hand side of Equation 2 is the contribution of thermal strain to the liquid pressure drop (ΔP_e), whereas the second term is the contribution from solidification shrinkage (ΔP_{sh}). The liquid flow v_L is calculated from Darcy's law:

$$f_L \cdot v_L = \frac{-K}{\mu} \frac{d(\Delta P_{sh} + \Delta P_e)}{dx} \quad (3)$$

with f_L : liquid fraction at the point of initial coherency.

Strain Partition Model. Defining how the local strain rate (across the mushy zone) is partitioned between grain boundaries is of particular importance to the crack growth model. Experimental local displacement measurements are typically made using an extensometer [32, 33] or LVDT [34] spanned across the mushy weld zone. Hence, it is convenient to consider this

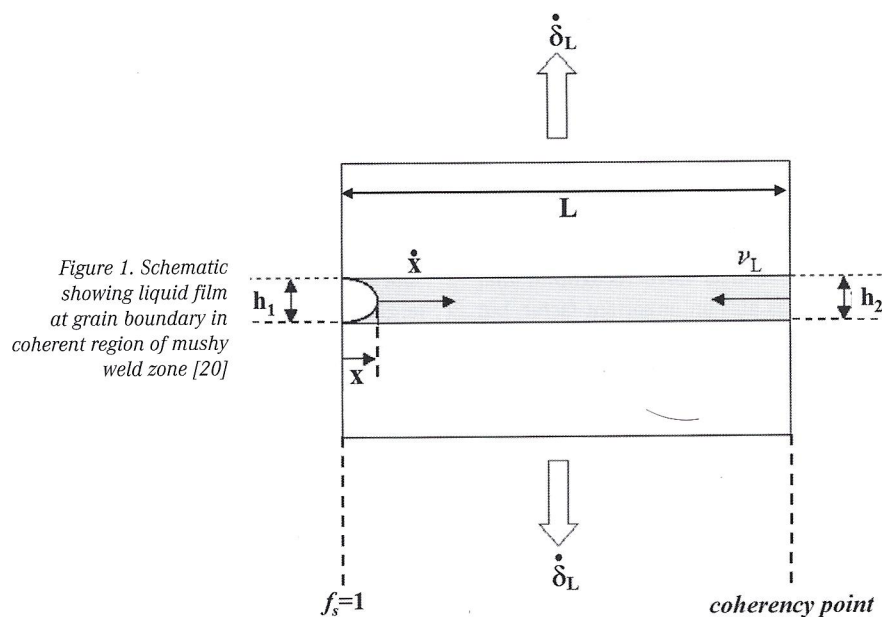


Figure 1. Schematic showing liquid film at grain boundary in coherent region of mushy weld zone [20]

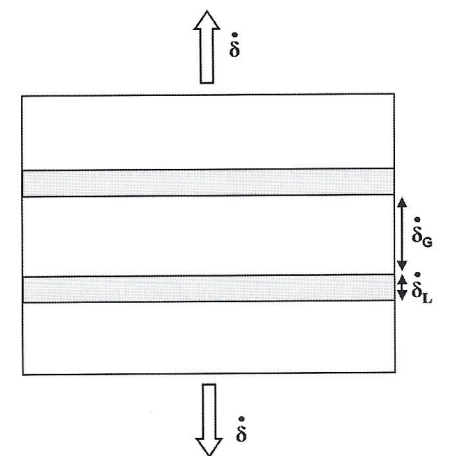


Figure 2. Scheme showing deformation rate across mushy zone ($\dot{\delta}$), grain ($\dot{\delta}_G$), and grain boundary liquid ($\dot{\delta}_L$) as defined in strain partition model of Equation (4)

measured local displacement rate ($\dot{\delta}$) as equally divided between N adjacent grains of equal size separated by liquid films of equal thickness using a very simple 2-D strain rate distribution model proposed in Figure 2 [25, 26]. The model assumes that grain coherency inside grains exceeds the coherency present at grain boundaries. Likewise, if a distinction is made between grain boundary liquid (δ_L) and grain (δ_G) displacement, the local displacement rate across the mushy zone (N grains) from Figure 2 can be given as [20]:

$$\dot{\delta} = N(\dot{\delta}_L + \dot{\delta}_G) \quad (4)$$

Similarly, the local strain rate across the mushy zone can be defined as:

$$\dot{\epsilon} = \dot{\delta}/W \quad (5)$$

with W : width of the mushy zone.

The deformation rate of grains in the mushy zone ($\dot{\delta}_G$) is approximately equal to the rate of solidification shrinkage $\dot{\delta}_{sh}$, and large in comparison to the deformation originating from the liquid pressure drop when considering aluminum alloys [20, 25, 26].

The thermal gradient G is assumed constant, thus the length L of the coherent zone (i.e., from coherency to solidus) can be estimated by:

$$L = \frac{T_{coh} - T_s}{G} \quad (6)$$

with T_{coh} and T_s : coherency and solidus temperatures. The time $\Delta t_{coh,s}$ for the temperature to drop from T_{coh} to T_s is related to the velocity of isotherms v_T (assumed equal to the welding speed):

$$\Delta t_{coh,s} = \frac{L}{v_T} \quad (7)$$

The solidification shrinkage rate $\dot{\delta}_{sh}$ is then determined by:

$$\dot{\delta}_{sh} = \frac{GS \cdot \beta \cdot (1 - f_{s,coh})}{\Delta t_{coh,s}} \quad (8)$$

with GS : grain size, $f_{s,coh}$: coherency solid fraction and β : linear solidification shrinkage factor.

Constants Used in Model Calculations. The present theoretical work investigates the effect of solidified weld metal grain size (average grain diameter), coherent temperature range, solid fraction at the coherency point, and solid fraction at the crack tip on the critical conditions to grow a crack at a

velocity equal to v_T . The values for constants utilized in model calculations are listed in Table 1. These values were selected, based upon a previous analysis [20], to represent approximate values for an aluminum alloy in general when welded using a gas tungsten arc process (490 J/mm heat input, 4 mm/s travel speed). While some values may vary for different aluminum alloys, these approximations are sufficient here for the purpose of establishing weldability trends. A volume shrinkage of 6% typical for aluminum is assumed, giving a linear shrinkage of 2%. The linear shrinkage is applied between the liquidus (T_L) and solidus (T_s) temperatures in proportion to the solid fraction.

Results

Model calculations focus on determining the effect of different metallurgical varia-

bles on the conditions required for crack growth. These conditions are expressed in terms of a critical grain boundary liquid deformation rate ($\dot{\delta}_{L,cr}$) and critical local strain rate ($\dot{\epsilon}_{cr}$), with larger (more positive) values indicating better weldability. Positive values represent outward displacement away from the weld center. The constants given in Table 1 will be kept constant except for one single metallurgical feature (e.g., CTR, GS, $f_{s,coh}$, $f_{s,CT}$) per investigation, which is purposely varied to examine and quantify its effect on weld solidification cracking susceptibility.

Coherent Temperature Range Effect. The coherent temperature range (CTR) was varied from 50 °C to 150 °C. The calculated values of $\dot{\delta}_{L,cr}$ and $\dot{\epsilon}_{cr}$ drop from $0.58 \mu\text{m} \times \text{s}^{-1}$ to $0.15 \mu\text{m} \times \text{s}^{-1}$ and $+0.07\% \times \text{s}^{-1}$ to $-0.80\% \times \text{s}^{-1}$, respectively, when increasing the CTR from 50 °C to 150 °C (Figure 3). Negative values of critical local strain rate

Parameter	Symbol	Value
Linear shrinkage factor	β	0.02
Liquid viscosity	μ	$1 \times 10^{-3} \text{ Pa} \times \text{s}$
Thermal gradient	G	$25,000 \text{ K} \times \text{m}^{-1}$
Velocity of isotherms	v_T	$0.004 \text{ m} \times \text{s}^{-1}$
Primary arm spacing	λ_1	$1 \times 10^{-5} \text{ m}$
Secondary arm spacing	λ_2	$1 \times 10^{-5} \text{ m}$
Permeability	K	$\frac{\lambda_2^2 \cdot (1 - f_s)^3}{180 \cdot f_s^2} \text{ m}^2$
Coherency temperature range	CTR	100 °C
Grain size	GS	50 μm
Solid fraction at coherency	$f_{s,coh}$	0.4
Solid fraction at crack tip	$f_{s,CT}$	0.98

Table 1. Values of constants used for calculations in Equations (1) to (8) from a previous publication [20] and from van Hoorn [35]

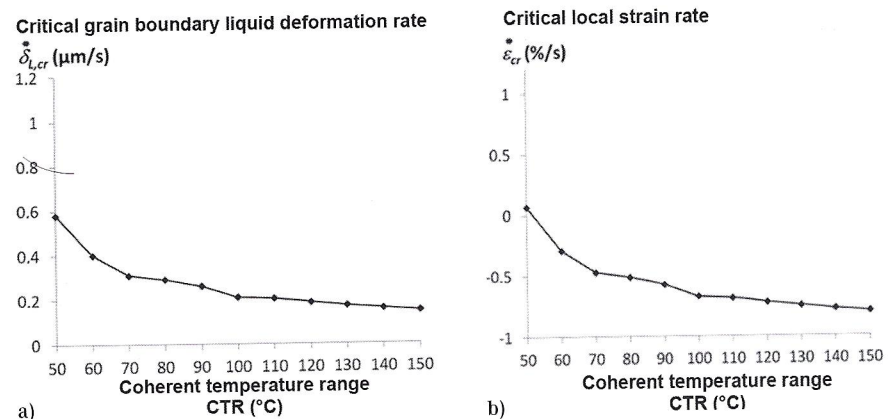


Figure 3. Effect of coherent temperature range (CTR) on a) minimum liquid deformation rate $\dot{\delta}_{L,cr}$ b) local strain rate $\dot{\epsilon}_{cr}$ to grow a continuous weld solidification crack

indicate inward movement of material and, accordingly, represent very poor weldability. Note that, in this case, the negative strain does not fully compensate for solidification shrinkage, allowing for a net sum tensile strain rate large enough to support crack growth.

This predicted loss in weldability with increased CTR follows the general concept that alloys with large coherent solidification ranges will experience higher cracking susceptibility due to difficulty in feeding shrinkage and the possibility to accumulate strain over longer solidification times. This Shrinkage-Brittleness theory was first proposed in the late 1940's [17, 31, 36, 37]. The model detailed in Equations (1) to (8) relates the solidification crack growth directly to the ability to feed transverse displacement in the mushy zone. This highlights the role of liquid supply provided in the mushy zone, with feeding becoming increasingly difficult with distance from the fusion line (i.e., closer to the solidus).

Another temperature range sometimes used to represent sensitivity to cracking is

the brittle temperature range (BTR) used empirically to predict relative cracking susceptibility of an alloy [38-40]. The BTR concept has been applied to establish characteristic ductility curves for specific aluminum alloys [15, 16, 41], defining a critical strain needed to cause cracking. However, it is not clear mechanistically what microstructural state the BTR represents. It is possible that BTR and CTR represent the same thing, i.e., range between coherency and solidus temperatures.

Grain Refinement Effect. The grain size (GS) value was varied from 10 μm to 150 μm . Calculated values of $\dot{\delta}_{L,cr}$ were unaffected by grain size, holding at a constant value of $0.21 \mu\text{m} \times \text{s}^{-1}$ (Figure 4a) per the mathematical formulation of Equation (1). However, a GS reduction from 150 μm to 10 μm increased the $\dot{\epsilon}_{cr}$ value from $-0.95 \% \times \text{s}^{-1}$ to $+1.01 \% \times \text{s}^{-1}$ (Figure 4b), and is associated with a change in the strain distribution across the mushy zone. Strain partitioning has received little attention [14, 20, 25, 26], despite its importance in relating experimental strain measurements to theory.

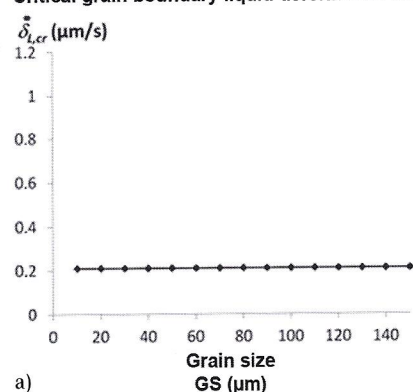
When considering the mushy zone, strain is localized in the most vulnerable region, i.e., at grain boundary liquid films, for temperatures below the coherency temperature.

Experimental investigations on aluminum alloys have shown a strong reduction in solidification cracking susceptibility with the addition of a grain refining element [42-45]. Grain size directly affects the strain distribution within the mushy zone; grain refinement increases the number of grain boundaries, thereby reducing the strain experienced by each boundary. Reduced cracking susceptibility of aluminum alloys AA7108 [45], AA6060 [42], Al-6 wt.-%Cu binary alloy [43], and Al-2.2Li-2.7Cu [44] with addition of grain refiners scandium [45], titanium boron, i.e., TiBor [42, 43, 45], titanium [44], and zirconium [44] have been related to grain refinement and the associated change from coarse columnar to refined equiaxed grain microstructure. Specific to this model, the beneficial role of grain refinement (i.e., large N in Equation (4)) in reducing cracking susceptibility [42-45] is associated with the lowering of the strain rate experienced at each single grain boundary.

Coherency Point Effect. The solid fraction at the coherency point ($f_{s,coh}$) was varied from 0.1 to 0.9, which reflects dendrite structure and what stage of solidification coherency begins. The calculated values of $\dot{\delta}_{L,cr}$ and $\dot{\epsilon}_{cr}$ were found to change from $0.29 \mu\text{m} \times \text{s}^{-1}$ to $0.19 \mu\text{m} \times \text{s}^{-1}$ and $-1.06 \% \times \text{s}^{-1}$ to $+0.20 \% \times \text{s}^{-1}$, respectively, when increasing $f_{s,coh}$ from 0.1 to 0.9 (Figure 5). The slight drop in $\dot{\delta}_{L,cr}$ reflects the difficulty in feeding liquid through narrower interdendritic channels associated with a greater solid fraction. On the other hand, the solidification shrinkage, assumed proportional to the solid fraction in Equation (8), is smaller for large $f_{s,coh}$ values. Therefore, while a higher coherency solid fraction hinders liquid feeding, this can be over-compensated by a large reduction in solidification shrinkage.

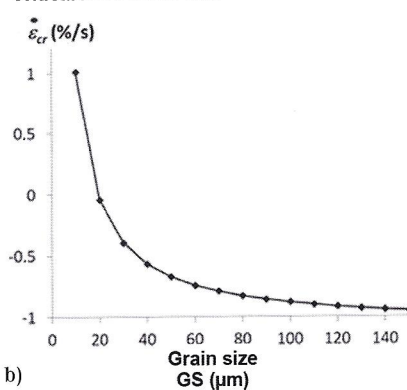
Crack Tip Location Effect. The location at which the crack tip grows, fixed in the mushy zone and expressed in terms of solid fraction ($f_{s,CT}$), is something that is not intrinsically known for any given alloy system and yet appears to be a key factor determining weldability. It is observed from the model that crack tip location can strongly reduce weldability if it is shifted to higher solid fractions. Calculated values of $\dot{\delta}_{L,cr}$ and $\dot{\epsilon}_{cr}$ change from $1.19 \mu\text{m} \times \text{s}^{-1}$ to $0.02 \mu\text{m} \times \text{s}^{-1}$ and $+1.27 \% \times \text{s}^{-1}$ to $-1.00 \% \times \text{s}^{-1}$, respectively, when increasing $f_{s,CT}$ from 0.9

Critical grain boundary liquid deformation rate



a)

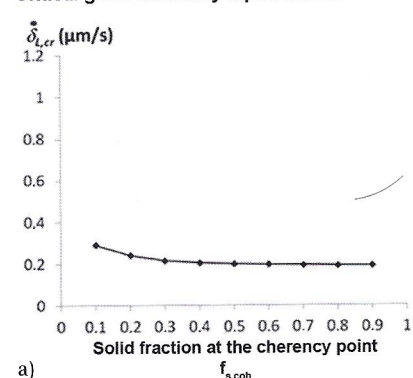
Critical local strain rate



b)

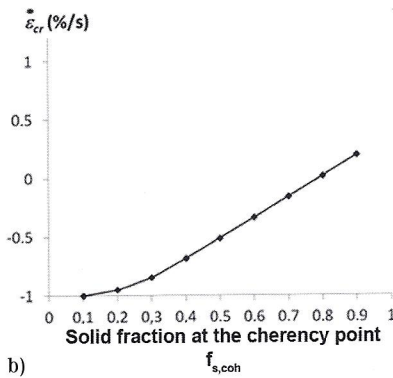
Figure 4. Effect of grain size (GS) on a) minimum liquid deformation rate $\dot{\delta}_{L,cr}$, b) local strain rate $\dot{\epsilon}_{cr}$ to grow a continuous weld solidification crack

Critical grain boundary liquid deformation rate



a)

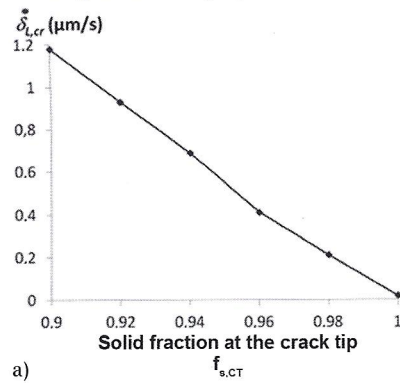
Critical local strain rate



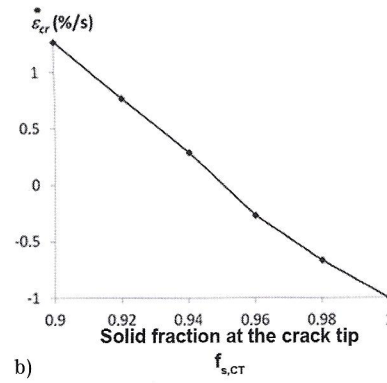
b)

Figure 5. Effect of solid fraction at coherency ($f_{s,coh}$) on a) minimum liquid deformation rate $\dot{\delta}_{L,cr}$, b) local strain rate $\dot{\epsilon}_{cr}$ to grow a continuous weld solidification crack

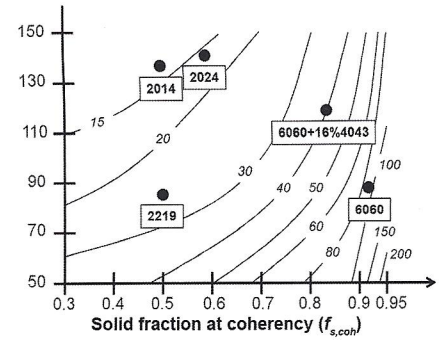
Critical grain boundary liquid deformation rate


 Figure 6. Effect of solid fraction at crack tip ($f_{s,CT}$) on a) minimum liquid deformation rate $\dot{\delta}_{L,cr}$ b) local strain rate $\dot{\epsilon}_{cr}$ to grow a continuous weld solidification crack

Critical local strain rate



Coherency temperature range CTR (°C)


 Figure 7. Calculated CTR: $f_{s,coh}$ map showing threshold grain size (in μm) in aluminum alloys to avoid weld solidification cracking under a local strain rate of $0.2\% \times \text{s}^{-1}$ and solid fraction at crack tip of 0.98

to 1.0 (Figure 6). This is a direct result of having to feed liquid over longer distances.

It can be argued that the crack tip will not locate at very low solid fractions where liquid can easily back-fill all voids. Voids simply cannot exist under these conditions and continuous crack growth is not possible. The crack tip also will not locate at very high solid fractions where liquid films become discontinuous. Here strength builds rapidly through dendrite bonding, as observed in tensile tests of semi-solid melts (typically at solid fractions above 0.96). Crack growth in this region would require solid-solid fracture, something not typically observed on solidification crack surfaces. Recall that the model specifically requires that a continuous liquid film be present and that the crack grow in the liquid.

Thus, it is likely that cracks will grow at or near the point of liquid discontinuity, avoiding any high energy breakage of solid-state bonds and yet releasing large amounts of strain energy as the centerline crack parts the weld. As with any steady state process, it is possible that the crack tip may drift ahead or behind its preferred growth location. Accordingly, some crack surfaces will occasionally show solid-solid breakage and sometimes indications of extensive liquid back-filling.

Discussion

One point of particular importance shown by model calculations is the overriding effect of grain refinement. The predicted weldability improvement at smaller grain size is in agreement with experimental data on weldability [42–46]. According to the present model, this important improvement may be explained by the synergy of

two consequences of grain refinement. First, grain refinement lowers the strain experienced by each individual grain boundary (recall Equation (4)). Second, grain refinement postpones the onset of strength buildup (i.e., coherency) during solidification [29]. This can be associated with a change in grain shape (columnar to equiaxed) and a greater degree of grain misorientation that comes with random crystal nucleation. In non-refined columnar structures, the large and highly branched grains inter-lock, hindering grain rearrangement, whereas in refined microstructures the small equiaxed grains more easily slide and adjust, resulting in a delayed development of strength. Moreover, a theoretical evaluation has shown that liquid film life is extended for highly misoriented adjacent grains [47]. Altogether, the consequent smaller grain size (GS) and increased solid fraction at coherency ($f_{s,coh}$) associated with grain refinement results in improved weldability (see Figures 4 and 5).

Also important is the location of the crack tip within the mushy zone, likely to be positioned just ahead of the onset of liquid discontinuity. This final stage of solidification involves the formation of isolated liquid pockets, which involves extensive inter-grain solid bridging and an associated increase in tensile strength [36, 37, 48]. Crack advancement in this region would require breakage of dendrites, which is not typically observed. Where this onset of liquid discontinuity occurs, key to locating the crack tip, is likely affected by dendrite structure and liquid properties. Solid bridging is dependent not only upon the quantity but also upon the distribution of liquid at the grain boundaries influenced by wettability [1, 36, 37, 49, 50].

The model suggests that all aluminum alloys can be made weldable as long as the weld metal grain size is below a critical value. This is of practical importance, because it means that a sufficient amount of grain refiner should be added to the filler metal to ensure that a critical weld metal grain size is achieved for a given alloy. The present model was used to generate the map shown in Figure 7 indicating the threshold grain size needed to avoid crack growth, shown as a function of CTR and $f_{s,coh}$ values, when submitted to a $0.2\% \times \text{s}^{-1}$ local strain rate. This map can be viewed as the envelope, i.e., surface, of the iso-strain rate plane at $0.2\% \times \text{s}^{-1}$ in a 3-D parametric space (grain size, CTR, $f_{s,coh}$). This map predicts that the best weldability is attained for aluminum alloys with small CTR and high $f_{s,coh}$.

The solidification paths for several commercial aluminum alloys (alloys 2014, 2024, 2219, and 6060), measured in previous study [28, 33], were used to locate each relative position of alloy on the map in Figure 7, assuming a constant $f_{s,CT}$ value of 0.98. It is observed that the position of at least one alloy, alloy 6060, does not fit with observed weldability behaviour as represented in the data of Table 2. Autogenous welds made on 6060 are known to be highly susceptible to solidification cracking, with improvements made using 4043 filler. This suggests that more accurate values for $f_{s,CT}$ are needed for each individual alloy. Also, the assumption of a constant strain rate ($0.2\% \times \text{s}^{-1}$) does not necessarily reflect the unique thermal mechanical response to welding for each alloy. Nevertheless, the concept demonstrated in Figure 7 presents a valuable tool for understanding weldability.

Due to the simplified nature of the model presented, not all factors that might affect sustained crack growth are accounted for. For example, the critical grain boundary liquid deformation rate could be affected by high temperature intermetallic phases that block the interdendritic liquid feeding path [54]. Also, a simplified dendritic solidification condition was assumed at the grain boundary, whereas the actual liquid film life at the grain boundary is predicted to be a function of misorientation of the adjacent grains [47]. The partitioning of thermal strain in the mushy zone must involve a complex interaction between grain morphology, coherency between grains, and grain boundary orientation relative to strain, with large stray grains along the center section contributing to poor weldability [33].

Summary

A comprehensive model that characterizes the underlying mechanisms involved in so-

lidification cracking in aluminum weldments has been used to map the conditions required for solidification crack growth by examining select metallurgical variables. These variables included coherent temperature range, grain size, solid fraction at coherency, and crack tip location. The model has proven useful in clarifying the role of these metallurgical features when applied to solidification crack growth.

In addition to reaffirming the previously established weldability improvements associated with grain refinement and smaller solidification temperature range, the model suggests that solid fraction at coherency is a major factor influencing weldability, where a delay in coherency sharply increases the minimum strain rate required for cracking. Likewise, where the crack tip resides, assumed to be near the onset of liquid discontinuity, is shown to have a major influence on weldability. The closer the crack tip is to the end of solidification, the more the weldability is lowered. This in-

sight on metallurgical factors can conceivably be applied to the development of alloys and filler metals having better weldability: small CTR, small grain size, high solid fraction at coherency, and rapid development of strength through solid-solid bonding should be optimized.

References

- 1 J. Campbell: Castings, Butterworth-Heinemann (1991)
- 2 R. A. Chihoski: The Character of Stress Field Around a Weld Arc Moving on Aluminum Sheet, Weld. J. 51 1 (1972), pp. 9s-18s
- 3 Z. Feng: A Computational Analysis of Thermal and Mechanical Conditions for Weld Metal Solidification Cracking, Welding in the World 33 (1994), pp. 340-347
- 4 T. Zacharia: Dynamic Stresses in Weld Metal Hot Cracking, Welding Journal 73 7 (1994), pp. 164s-172s
- 5 D. G. Eskin, L. Katgerman: A Quest for a New Hot Tearing Criterion, Met. Mat. Trans. 38A 7 (2007), pp. 1511-1519
- 6 D. G. Eskin, W. H. Kool, L. Katgerman: Hot Tearing Criteria Evaluation for Direct-Chill Casting of an Al-4.5 Pct Cu Alloy, Met. Mat. Trans. 36A 6 (2005), pp. 1537-1546
- 7 C. E. Cross: On the Origin of Weld Solidification Cracking, T. Böllinghaus, H. Herold (Eds.), Hot Cracking Phenomena in Welds, Springer Pub (2005), pp. 3-18
- 8 D. G. Eskin, W. H. Suyitno, L. Katgerman: Mechanical Properties in the Semi-Solid State and Hot Tearing of Aluminum Alloys, Prog. Mat. Sci. 49 (2004), pp. 629-711
- 9 C. E. Cross, N. Coniglio: Weld Solidification Cracking: Critical Conditions for Crack Initiation and Growth, T. Böllinghaus, H. Herold, C. E. Cross, J. C. Lippold (Eds.), Hot Cracking Phenomena in Welds II, Springer (2008), pp. 39-58
- 10 N. Coniglio, C. E. Cross: Initiation and Growth Mechanisms for Weld Solidification Cracking, Int. Mat. Rev. 58 7 (2013), pp. 375-397 DOI:10.1179/1743280413Y.0000000020
- 11 V. N. Saveiko: Theory for Hot Cracking, Russ. Cast. Prod. (1961), pp. 453-456
- 12 C. H. Dickhaus, L. Ohm, S. Engler: Mechanical Properties of Solidifying Shells of Aluminum Alloys, AFS Trans. 101 (1994), pp. 677-684
- 13 D. J. Lahaie, M. Bouchard: Physical Modeling of the Deformation Mechanisms of Semi-Solid Bodies and a Mechanical Criterion for Hot Tearing, Met. Mat. Trans. 32B 8 (2001), pp. 697-705
- 14 W. S. Pellini: Strain Theory for Hot Tearing, Foundry 80 (1952), pp. 125-199
- 15 N. N. Prokhorov: The Problem of the Strength of Metals While Solidifying During Welding, Svar. Proiz. 6 (1956), pp. 5-11
- 16 T. Senda, F. Matsuda, G. Takano, K. Watanabe, T. Kobayashi, T. Matsuzaka: Experimental Investigations on Solidification Crack Susceptibility for Weld Metals with Trans-Varestraint Test, Trans. JWS 2 2 (1971), pp. 141-162
- 17 W. I. Pumphrey, P. H. Jennings: A Consideration of the Nature of Brittleness and Tempera-

Material base metal + filler metal)	Welding conditions			Weldability test*	Critical strain rate (%/s)	Reference
	Voltage (V)	Current (A)	Welding speed (mm/s)			
Al alloy 1050	25	200	2.5	TVT	7.5	[16]
Al alloy 1070	-	-	1.7	SB-TVT	5.00	[51]
Al alloy 2017	18	230	1.7	SB-TVT	0.20	[52]
Al alloy 2017	-	-	1.7	SB-TVT	0.15	[51]
Al alloy 2024	25	200	2.5	TVT	0.72	[16]
Al alloy 2219	-	-	1.7	SB-TVT	0.50	[51]
Al alloy 5052	-	-	5	VTST	0.15	[53]
Al alloy 5052	-	-	1.7	SB-TVT	0.64	[51]
Al alloy 5083	25	200	2.5	TVT	0.15	[16]
Al alloy 5083	18	230	1.7	SB-TVT	0.35	[51]
Al alloy 5083	-	-	5	VTST	0.20	[53]
Al alloy 5083	-	-	1.7	SB-TVT	0.47	[51]
Al alloy 5154	-	-	1.7	SB-TVT	0.70	[51]
Al alloy 6060	17.8	110	4	CTW	-0.06	[33]
Al alloy 6060+5%4043	17.8	110	4	CTW	0.06	[33]
Al alloy 6060+9%4043	17.8	110	4	CTW	0.17	[33]
Al alloy 6060+11%4043	17.8	110	4	CTW	0.22	[33]
Al alloy 6060+14%4043	17.8	110	4	CTW	0.30	[33]
Al alloy 6060+16%4043	17.8	110	4	CTW	0.35	[33]

* TVT = transvarestraint test, SB-TVT = slow bending trans varestraint test, CTW = controlled tensile test, VTST = variable tensile strain test, VDRT = variable deformation rate test

Table 2. Relative aluminum alloy weldability expressed as critical strain rate required for weld solidification crack formation

- ture Above the Solidus in Castings and Welds in Aluminum Alloys, *J. Inst. Metals* 75 (1948), pp. 235-256
- 18 J. C. Borland: Generalized Theory of Super Solidus Cracking in Welds and Castings - an Initial Development, *Brit. Weld. J.* 8 (1961), pp. 526-540
 - 19 M. Rappaz, J.-M. Drezet, M. Gremaud: A New Hot-Tearing Criterion, *Met. Mat. Trans.* 30A (1999), pp. 449-455
 - 20 N. Coniglio, C. E. Cross: Mechanisms for Solidification Crack Initiation and Growth in Aluminum Welding, *Met. Trans.* 40A (2009), pp. 2718-2728
DOI: 10.1007/s11661-009-9964-4.
 - 21 H. Murakawa, H. Serizawa, M. Shibahara: Prediction of Welding Hot Cracking Using Temperature Dependent Interface Element, H. Cerjak, H. K. D. H. Bhadeshia, E. Kozeschnik (Eds.), *Mathematical Modeling of Weld Phenomena* 7, Maney (2003), pp. 539-554
 - 22 J. A. Williams, A. R. E. Singer: Deformation, Strength, and Fracture Above the Solidus Temperature, *J. Inst. Metals* 96 (1968), pp. 5-12
 - 23 D. G. Suyitno, W. H. Kool, L. Katgerman: Micro-Mechanical Model of Hot Tearing at Triple Junctions in DC Casting, *Mat. Sci. Forum* 396-402 (2002), pp. 179-184
 - 24 J. F. Grandfield, C. J. Davidson, J. A. Taylor: Application of a New Hot Tearing Analysis to Horizontal Direct Chill Cast Magnesium Alloy AZ91, J. L. Anjier (Ed.), *Light Metals* 2001, Warrendale TMS (2001), pp. 895-901
 - 25 M. Braccini, C. L. Martin, M. Suéry, Y. Bréchet: Relation Between Mushy Zone Rheology and Hot Tearing Phenomena in Al-Cu Alloys, P. B. Sahn, P. N. Hansen, J. G. Conley (Eds.), *Modeling of Casting, Welding, and Advanced Solidification Processes IX*, Shaker Verlag Aachen (2000), pp. 19-24
 - 26 M. Braccini, C. L. Martin, M. Suéry, Y. Bréchet: Hot Tearing Phenomena in Al-Cu Alloys, *Matériaux et Techniques* 5-6 (2000), pp. 19-24
 - 27 C. V. Robino, M. Reece, G. A. Knorovsky, J. N. DuPont, Z. Feng: Prediction of Maximum Crack Length in Longitudinal Vastrestaint Testing, S. A. David (Ed.), *Proc. 7th Int. Conf. Trends in Welding Research*, ASM Int. (2005), pp. 313-318
 - 28 C. E. Cross, N. Coniglio, P. Schempp, M. Mousavi: Critical Conditions for Weld Solidification Crack Growth, J. Lippold, T. Böllinghaus, C. E. Cross (Eds.), *Hot Cracking Phenomena in Welds III*, Springer Verlag Berlin Heidelberg (2011), pp. 25-41
 - 29 A. K. Dahle, L. Arnberg: Development of Strength in Solidifying Aluminum Alloys, *Acta Mater.* 45 (2) (1997), pp. 547-559
 - 30 L. Bäckerud, E. Krol, J. Tamminen: Solidification Characteristics of Aluminum Alloys, Vol. 1, Skanalumium, Oslo (1986).
 - 31 A. R. E. Singer, S. A. Cottrell: Properties of the Aluminum-Silicon Alloys at Temperatures in the Region of the Solidus, *J. Inst. of Metals* 73 (1947), pp. 33-54
 - 32 T. Kannengiesser, T. McInerney, W. Florian, T. Böllinghaus, C. E. Cross: The Influence of Local Weld Deformation on Hot Cracking Susceptibility, H. Cerjak (Ed.), *Mathematical*

Abstract

Kohärenz- und Korngrößeneffekte auf das Erstarrungsrissswachstum in Aluminiumschweiß-Verbindungen. In dem vorliegenden Beitrag wird ein Massenbilanzmodell evaluiert, das die kritischen Bedingungen für anhaltendes kontinuierliches Rissswachstum in der weichen Schweißnahtzone abschätzt. Mit Hilfe eines Dehnungs-Teilungs-Modells wurde die kritische lokale Dehnrate (über dem Querschnitt der Schweißnaht) ins Verhältnis zur kritischen Korngrenzendeformationsrate gesetzt, die für Rissswachstum erforderlich ist. In der vorliegenden Arbeit wurden diese beiden Modelle auf Aluminiumschweißungen angewendet, um die theoretischen Effekte von verschiedenen metallurgischen Faktoren auf die Erstarrungsrisssanfälligkeit zu untersuchen. Die Berechnungen quantifizieren den verbesserten Risswiderstand, der mit einem kleineren Kohärenz-Temperaturbereich, der Kornfeinung, dem hohen Festanteil bei Kohärenz, und der rapiden Entwicklung der Zugfestigkeit durch Fest-Fest-Bindung einhergeht.

Modeling of Weld Phenomena 6, Maney (2002), pp. 803-817

- 33 N. Coniglio, C. E. Cross, T. Michael, M. Lammers: Defining a Critical Weld Dilution to Avoid Solidification Cracking in Aluminum, *Weld. J.* 87 (8) (2008), pp. 237s-247s
- 34 H. Herold, M. Streitenberger, A. Pchennikov: Modeling of the PVR Test to Examine the Origin of Different Hot Cracking Types, H. Cerjak (Ed.), *Mathematical Modelling of Weld Phenomena* 5, IOM London (2001), pp. 783-792
- 35 K. R. Van Horn: Aluminum, Vol. 1: Properties, Physical Metallurgy, and Phase Diagrams, ASM, Metals Park, OH (1967)
- 36 A. R. E. Singer, P. H. Jennings: Hot Shortness of the Aluminum-Silicon Alloys of Commercial Purity, *J. Inst. of Metals* 73 (1947), pp. 197-212
- 37 J. Verö: The Hot-Shortness of Aluminum Alloys, *The Metal Industry* 48 (1936), pp. 431-494
- 38 J. C. Borland: Generalized Theory of Super Solidus Cracking in Welds and Castings - an Initial Development, *Brit. Weld. J.* 7 (8) (1960), pp. 508-512
- 39 F. Matsuda, H. Nakagawa, K. Sorada: Dynamic Observation of Solidification and Solidification Cracking during Welding with Optical Microscope (I) - Solidification Front and Behaviour of Cracking, *Trans. of JWRI* 11 (2) (1982), pp. 67-77
- 40 B. I. Medovar: On the Nature of Weld Hot Cracking, *Automat. Svarka* 7 (1954), pp. 12-28
- 41 F. Matsuda, K. Nakata, K. Tsukamoto, T. Uchiyama: Effect of Additional Element on Weld Solidification Crack Susceptibility of Al-Zn-Mg Alloy (Report III), *Trans. of JWRI* 13 (1984), pp. 57-66
- 42 N. Coniglio, C. E. Cross: Weld Parameter and Minor Element Effects on Solidification Crack Initiation in Aluminium, T. Böllinghaus, H. Herold, C. E. Cross, J. C. Lippold (Eds.), *Hot Cracking Phenomena in Welds II*, Springer (2008), pp. 277-310
- 43 N. Coniglio, C. E. Cross: Towards Establishment of Standards for Weldability Testing For Solidification Cracking, T. Böllinghaus, J. C. Lippold, C. E. Cross, (Eds.), *Hot Cracking Phenomena in Welds IV*, Springer (2014), in press
- 44 M. J. Dvornak, R. H. Frost, D. L. Olson: The Weldability and Grain Refinement of Al-2.2Li-2.7Cu, *Weld. J.* 68 (8) (1989), pp. 327s-337s
- 45 M. G. Mousavi, C. E. Cross, Ø. Grong: Effect of Scandium and Titanium-Boron on Grain Refinement and Hot Cracking of Aluminum Alloy 7108, *Sci. Tech. Weld. Joining* 4 (6) (1999), pp. 381-388
- 46 S. Lin, C. Aliravci, M. O. Pekguleryuz: Hot-Tear Susceptibility of Aluminum Wrought Alloys and the Effect of Grain Refining, *Met. Mat. Trans.* 38A (2007), pp. 1056-1068
DOI:10.1007/s11661-007-9132-7
- 47 M. Rappaz, A. Jacot, W. J. Boettinger: Last-Stage Solidification of Alloys: Theoretical Model of Dendrite-Arm and Grain Coalescence, *Met. Mat. Trans.* 34A (3) (2003), pp. 467-479

- 48 W. M. van Haaften, W. H. Kool, L. Katgerman: Tensile Behaviour of Semi-Solid Industrial Aluminum Alloys AA3104 and AA5182, *Mat. Sci. Eng. A336* (2002), pp. 1-6
- 49 T. W. Clyne, G. J. Davies: Comparison between Experimental Data and Theoretical Predictions relating to Dependence of Solidification Cracking on Composition, *Proc. Int. Conf. Solidification*, Sheffield, 1977, *The Metals Society Book 192*, London, 1979, pp. 275-278
- 50 G. K. Sigworth: Hot Tearing of Metals, *AFS Trans.* 104 (1996), pp. 1053-1062
- 51 Y. Arata, F. Matsuda, K. Nakata, K. Shinozaki: Solidification Crack Susceptibility of Aluminum Alloy Weld Metals (Report II) - Effect of Straining Rate on Cracking Threshold in Weld Metal During Solidification, *Trans. of JWRI* 6 (1) (1977), pp. 91-104
- 52 Y. Arata, F. Matsuda, K. Nakata, K. Shinozaki: Solidification Crack Susceptibility of Aluminum Alloy Weld Metals (Report III) - Effect of Straining Rate on Crack Length in Weld Metal, *Trans. of JWRI* 6 (2) (1977), pp. 47-52
- 53 H. Tamura, N. Kato, S. Ochiai, Y. Katagiri: Cracking Study of Aluminum Alloys by the Variable Tensile Strain Hot Cracking Test, *Trans. JWS* 8 (2) (1977), pp. 16-22
- 54 M. G. Mousavi, C. E. Cross, Ø. Grong: The Effect of High-Temperature Eutectic-Forming Impurities on Aluminum 7108 Weldability, *Weld. J.* 88 (5) (2009), pp. 104s-110s

Bibliography

DOI 10.3139/120.110599
Materials Testing
56 (2014) 7-8, pp. 583-590
© Carl Hanser Verlag GmbH & Co. KG
ISSN 0025-5300

The Authors of This Contribution

Dr. Nicolas Coniglio is instructor at Ecole Nationale Supérieure d'Arts et Métiers, MSMP Laboratory, in Aix en Provence, France. He did his undergraduate studies at University of Nantes (France) and received his Dr.-Ing. degree from Otto von Guericke University (Germany), while working at Bundesanstalt für Materialforschung und Prüfung in Berlin. He did post-doctoral work at the University of Adelaide (Australia) and at the CNRC-CTA laboratory in Quebec (Canada).

Dr. Carl E. Cross is staff scientist in materials science and technology at the Los Alamos National Laboratory in Los Alamos, New Mexico (USA). He received undergraduate and graduate degrees in metallurgical engineering from the Colorado School of Mines, USA. Prior positions have included senior scientist at BAM, associate professor at Montana Tech of the University of Montana, and welding engineer at Martin Marietta Astronautics and Rockwell International. He also held post-doc positions at Helmut Schmidt University in Hamburg and NTNU in Trondheim.